Supplementary Materials

Fabrication and Comprehensive Evaluation of Zr-Based Bulk Metallic Glass Matrix Composites for Biomedical Applications

Mariusz Hasiak, Beata Sobieszczańska, Amadeusz Łaszcz, Michał Biały, Jacek Chęcmanowski, Tomasz Zatoński*

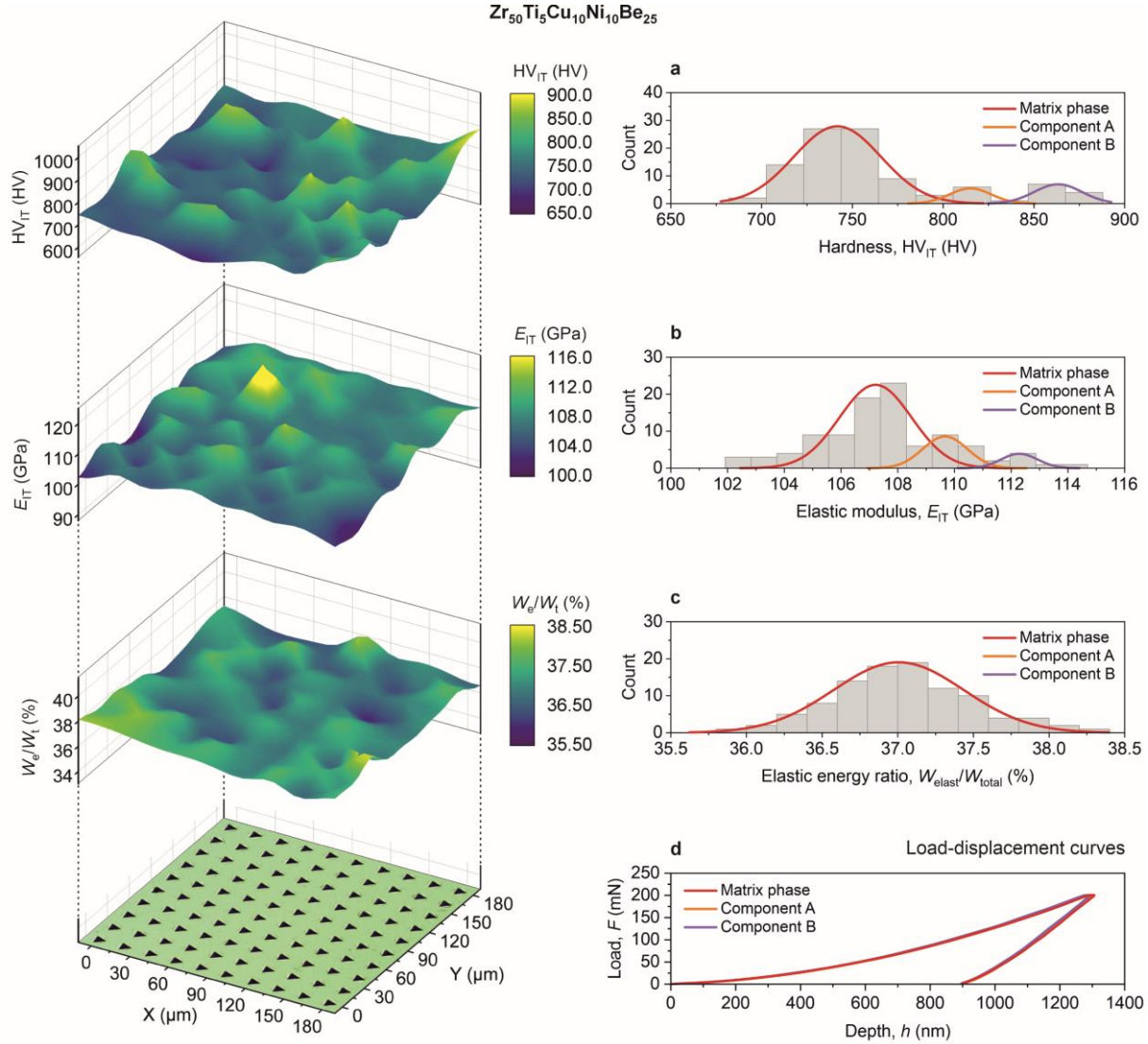

Fig. S1. Nanoindentation mapping of mechanical parameters rendered in the form of heatmaps (left) with corresponding (right) distributions of (a) instrumented hardness, HV_{IT}, (b) instrumented elastic modulus, E_{IT}, (c) elastic energy ratio, W_e/W_t, and (d) load-displacement curves for the $Zr_{50}Ti_5Cu_{10}Ni_{10}Be_{25}$ alloy.

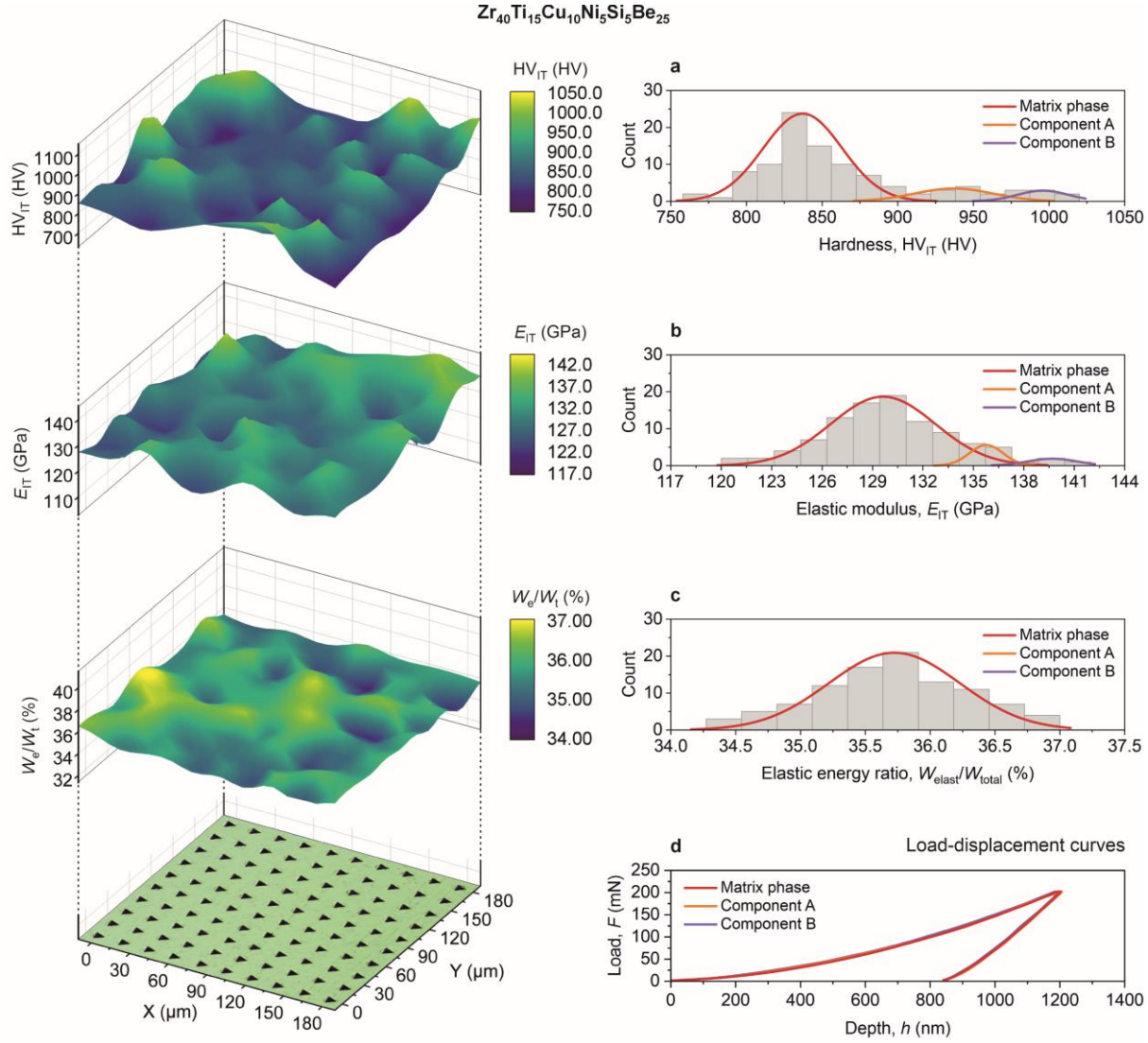

Fig. S2. Nanoindentation mapping of mechanical parameters rendered in the form of heatmaps (left) with corresponding (right) distributions of (a) instrumented hardness, HV_{IT}, (b) instrumented elastic modulus, E_{IT}, (c) elastic energy ratio, W_e/W_t, and (d) load-displacement curves for the $Zr_{40}Ti_{15}Cu_{10}Ni_5Si_5Be_{25}$ alloy.

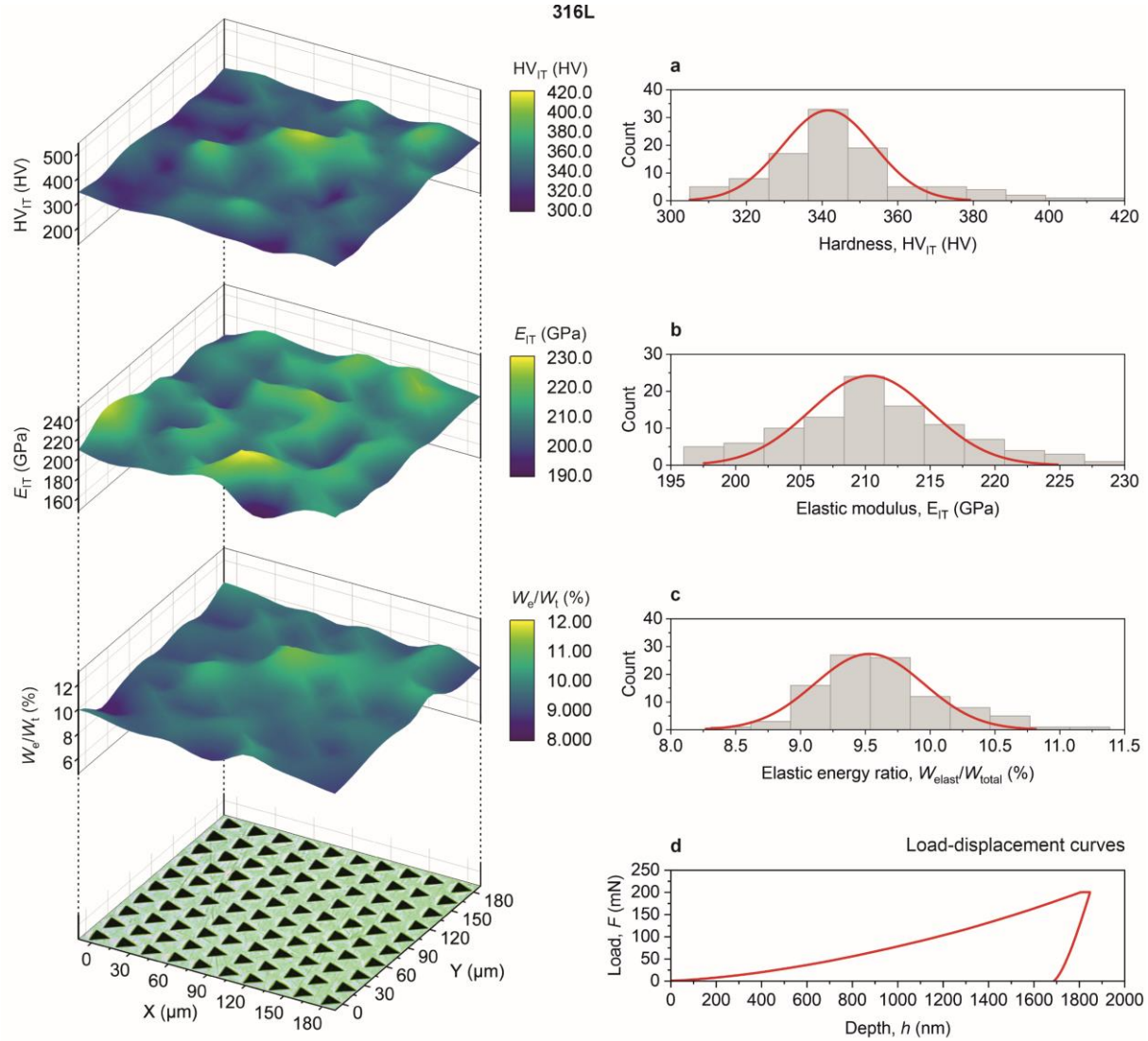

Fig. S3. Nanoindentation mapping of mechanical parameters rendered in the form of heatmaps (left) with corresponding (right) distributions of (a) instrumented hardness, HV_{IT}, (b) instrumented elastic modulus, E_{IT}, (c) elastic energy ratio, W_e/W_t, and (d) load-displacement curves for the 316L stainless steel.

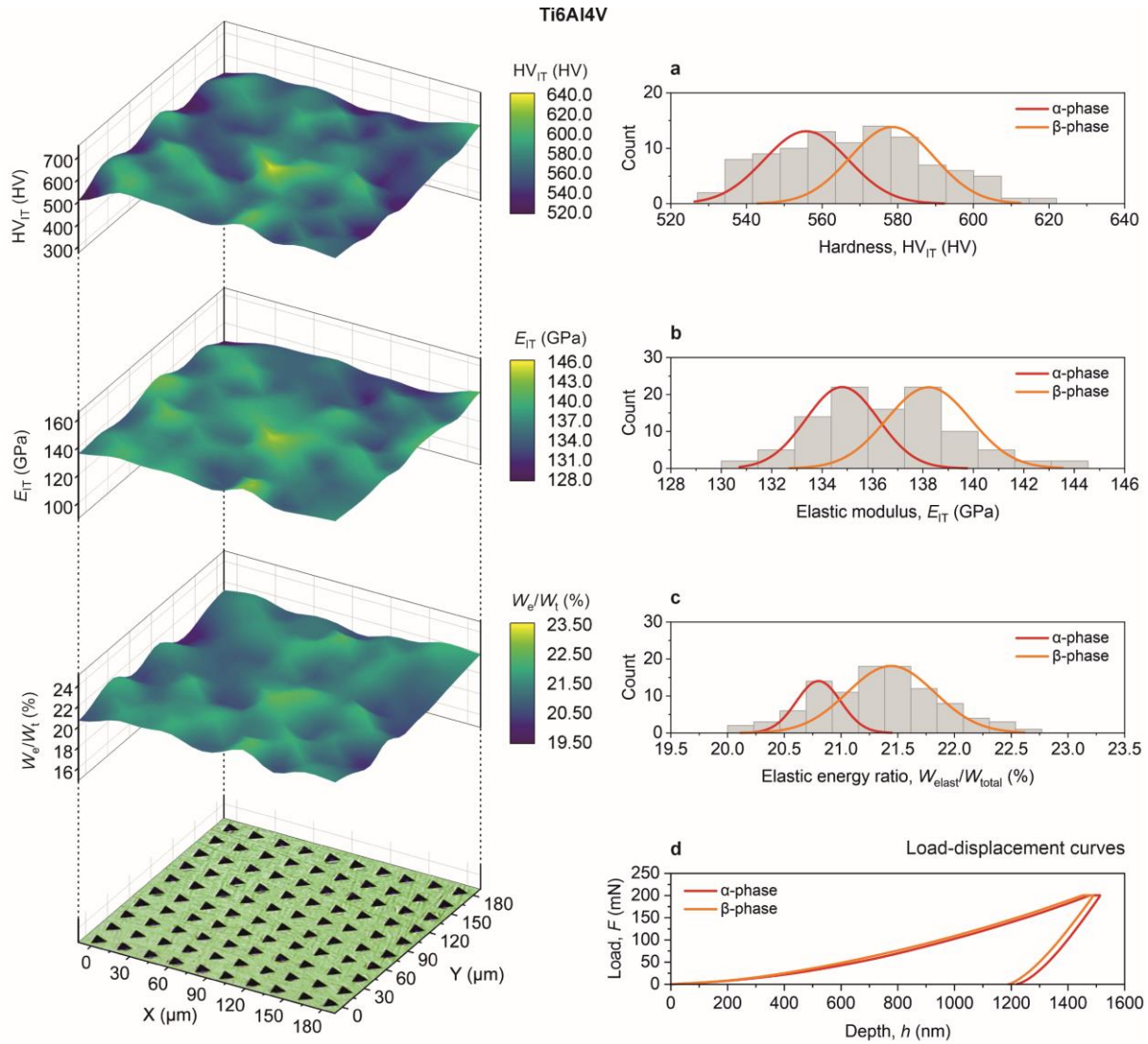

Fig. S4. Nanoindentation mapping of mechanical parameters rendered in the form of heatmaps (left) with corresponding (right) distributions of (a) instrumented hardness, HV_{IT}, (b) instrumented elastic modulus, E_{IT}, (c) elastic energy ratio, W_e/W_t, and (d) load-displacement curves for the Ti6Al4V alloy.

Table S1. Polarization resistance (R_p), corrosion current density (i_{corr}), cathodic to anodic transition potential ($E_{C\text{-}A}$), and open circuit potential (E_{OC}) for the fabricated $Zr_{40}Ti_{15}Cu_{10}Ni_{10}Be_{25}$, $Zr_{50}Ti_5Cu_{10}Ni_{10}Be_{25}$, and $Zr_{40}Ti_{15}Cu_{10}Ni_5Si_5Be_{25}$ BMG-MCs as well as reference 316L stainless steel and Ti6Al4V alloy recorded in the stability region between 5 and 42 days of exposure in SBF

Alloy	Time [days]	R_p [Ω cm^2]	i_{corr} [A cm^{-2}]	$E_{C\text{-}A}$ [mV]	E_{OC} [mV]
$Zr_{40}Ti_{15}Cu_{10}Ni_{10}Be_{25}$	5	$2.27 \cdot 10^5$	$1.15 \cdot 10^{-8}$	−612	−123
	13	$3.28 \cdot 10^5$	$7.95 \cdot 10^{-8}$	−666	−134
	22	$2.64 \cdot 10^5$	$9.86 \cdot 10^{-8}$	−588	−76
	42	$7.29 \cdot 10^5$	$3.58 \cdot 10^{-8}$	−308	+10
$Zr_{50}Ti_5Cu_{10}Ni_{10}Be_{25}$	5	$2.72 \cdot 10^5$	$9.81 \cdot 10^{-8}$	−627	−91
	13	$4.88 \cdot 10^4$	$5.34 \cdot 10^{-7}$	−636	−151
	22	$3.96 \cdot 10^5$	$6.59 \cdot 10^{-8}$	−511	−180
	42	$2.36 \cdot 10^5$	$1.11 \cdot 10^{-7}$	−421	−7
$Zr_{40}Ti_{15}Cu_{10}Ni_5Si_5Be_{25}$	5	$1.49 \cdot 10^5$	$1.70 \cdot 10^{-7}$	−562	−125
	13	$2.36 \cdot 10^5$	$1.11 \cdot 10^{-7}$	−564	−81
	22	$2.61 \cdot 10^5$	$1.05 \cdot 10^{-7}$	−604	−146
	42	$3.22 \cdot 10^5$	$8.09 \cdot 10^{-8}$	−346	−262
Ti6Al4V	5	$2.47 \cdot 10^5$	$2.63 \cdot 10^{-7}$	−478	−472
	13	$2.13 \cdot 10^5$	$2.66 \cdot 10^{-7}$	−483	−487
	22	$2.47 \cdot 10^5$	$3.24 \cdot 10^{-7}$	−533	−476
	42	$2.47 \cdot 10^5$	$1.26 \cdot 10^{-7}$	−593	−599
316L	5	$3.31 \cdot 10^4$	$7.74 \cdot 10^{-7}$	−303	−207
	13	$3.34 \cdot 10^4$	$7.81 \cdot 10^{-7}$	−328	−199
	22	$4.42 \cdot 10^4$	$5.90 \cdot 10^{-7}$	−352	−196
	42	$4.57 \cdot 10^4$	$5.72 \cdot 10^{-7}$	−325	−187